FERMILAB-CONF-16-386-PPD & CDF Note 11206 & D0 Note 6492

Forward-backward asymmetries in top-antitop quark production at the Tevatron

CDF and D0 Collaborations

September 20, 2016

Abstract

We present the combined results on inclusive forward-backward asymmetries in the production of top-antitop quark pairs and their decay leptons. The analysis is based on measurements by the CDF and D0 experiments at the Fermilab $p\overline{p}$ Tevatron collider using all the data collected at $\sqrt{s} = 1.96$ TeV. The measured asymmetries are in agreement with standard model predictions.

1 Introduction

The production of $t\bar{t}$ pairs in $p\bar{p}$ collisions can result in a difference in forward and backward cross sections of top or antitop quarks, where forward-produced top quarks (or forward antitop quarks) are defined as those with positive projections of their momenta along the proton (or antiproton) beam direction, and vice versa for backward-produced quarks. In the standard model (SM), the forward-backward asymmetries are zero in leading order (LO) quantum chromodynamics, but at next-to-leading order (NLO) and above, positive contributions to the asymmetry from the interference of LO and higher order diagrams, and smaller negative contributions from the interference of initial and final state radiations, lead to a prediction of an overall positive asymmetry [1, 2].

The CDF [3] and D0 [4] experiments have measured forward-backward asymmetries, culminating in studies using all the Tevatron Run II data. Both experiments have measured asymmetries for events in the single-lepton + jets channel (where one W boson from a top quark decays to a lepton and a neutrino, and the other decays to $q\bar{q}'$ that evolve to jets), and events in the dilepton channel (where both W bosons decay leptonically). While previous measurements exhibited some inconsistency with then-existing SM predictions, the final measurements and more refined predictions are in better agreement [5]. In this note we summarize the combination of the final CDF and D0 measurements and compare them with current SM calculations.

For reconstructed t and $\bar{t}$ quarks, the $t\bar{t}$ asymmetry $A_{\rm FB}^{t\bar{t}}$ is defined by:

$$A_{\rm FB}^{t\bar{t}} = \frac{N(\Delta y_{t\bar{t}} > 0) - N(\Delta y_{t\bar{t}} < 0)}{N(\Delta y_{t\bar{t}} > 0) + N(\Delta y_{t\bar{t}} < 0)} \quad , \tag{1}$$

where $\Delta y_{t\bar{t}} = y_t - y_{\bar{t}}$ is the rapidity difference between the t and $\bar{t}$ quark and N is the number of events in a particular configuration.

The asymmetry in t and $\bar{t}$ quark production also leads to asymmetries in their decay leptons. The single lepton asymmetry, $A_{\rm FB}^{\ell}$, is defined by:

$$A_{\rm FB}^{\ell} = \frac{N(q_\ell \eta_\ell > 0) - N(q_\ell \eta_\ell < 0)}{N(q_\ell \eta_\ell > 0) + N(q_\ell \eta_\ell < 0)} \quad , \tag{2}$$

where q_ℓ is the electric charge sign and η_ℓ is the pseudorapidity of the lepton in the laboratory frame.

For the dilepton channel, a dilepton asymmetry $A_{\rm FB}^{\ell\ell}$ is defined as:

$$A_{\rm FB}^{\ell\ell} = \frac{N(\Delta\eta > 0) - N(\Delta\eta < 0)}{N(\Delta\eta > 0) + N(\Delta\eta < 0)} \quad , \tag{3}$$

where $\Delta\eta$ is the pseudorapidity difference between the ℓ^+ and ℓ^-.

Measurements of $A_{\rm FB}^{t\bar{t}}$ by CDF and D0 were reported in Refs. [6, 7] for the lepton + jets channel and in Refs. [8, 9] for the dilepton channel. Measurements of $A_{\rm FB}^{\ell}$ are found in Refs. [11, 12] and in the dilepton channel in Refs. [13, 14]. Measurements of $A_{\rm FB}^{\ell\ell}$ are in Refs. [13, 14].

We combine the CDF and D0 inclusive asymmetries $A_{\rm FB}^{t\bar{t}}$, $A_{\rm FB}^{\ell}$ and $A_{\rm FB}^{\ell\ell}$ using the Best Linear Unbiased Estimator (BLUE) method [15–17]. All of the inclusive asymmetries are extrapolated to the full phase space. The differential measurements of the $A_{\rm FB}^{t\bar{t}}$ asymmetries as a function of $|\Delta y|$ and as a function of the mass of the $t\bar{t}$ system ($m_{t\bar{t}}$), the differential $A_{\rm FB}^{\ell}$ asymmetry as a function of $q_\ell \eta_\ell$, and the differential $A_{\rm FB}^{\ell\ell}$ asymmetry as a function of $\Delta\eta$ are not combined, but are plotted together to provide a comparison.

2 Systematic uncertainties and correlations

We have standardized and combined individual CDF and D0 systematic uncertainties into several categories: background modeling, signal modeling, detector response, method, and parton distribution functions (PDF). The correlations of systematic uncertainties among the analysis channels and between experiments for these categories are taken as specified below.

(i) "Background" - the uncertainties in contributions from background distributions and their normalizations are assumed to be uncorrelated since the backgrounds are estimated differently in different analyses and in the two experiments.

(ii) "Signal" - the uncertainties in modeling the signal, parton shower, initial and final state radiation, and color connections are taken as fully correlated between analyses and experiments because they all contain the same assumptions and potential systematic biases.

(iii) "Detector" - the uncertainties in jet energy scale and the modeling of the detector are correlated within an experiment but uncorrelated between experiments.

(iv) "Method" - the uncertainties in the chosen method of correcting for detector acceptance, efficiency, and potential biases in the reconstruction of top quark kinematic properties. In most cases, the uncertainties on corrections and unfolding procedures are taken to be uncorrelated. However, the uncertainties on the phase space correction procedures for the leptonic asymmetry in the D0 lepton + jet and dilepton analyses are estimated using the same methods and are therefore fully correlated.

(v) "PDF" - the uncertainties in the PDF and the pileup in energy from overlapping $p\bar{p}$ interactions are treated as fully correlated because they characterize the same potential systematic biases across all analyses.

In the case of correlated uncertainties, we assume that the correlation is 100%.

3 $A_{\mathrm{FB}}^{t\bar{t}}$ combination

The uncertainties in each of the $A_{\mathrm{FB}}^{t\bar{t}}$ measurements are summarized in Table 1. The CDF and D0 $A_{\mathrm{FB}}^{t\bar{t}}$ input values and their combination using BLUE in the ℓ + jets and dilepton channels are shown in Table 2, together with the statistical, systematic, and total uncertainties, as well as the weights from each measurement contributing to the combination. The resulting $A_{\mathrm{FB}}^{t\bar{t}} = 0.128 \pm 0.025$ has a χ^2 of 1.74 for 3 degrees of freedom, for a probability of 63%, which is consistent within 1.3 standard deviations with the next-to-NLO (NNLO) SM prediction of 0.095 ± 0.007 [1].

Table 1: The statistical and systematic uncertainties in the individual $A_{\mathrm{FB}}^{t\bar{t}}$ inputs.

Uncertainty	CDF ℓ+jets [6]	CDF dilepton [9]	D0 ℓ+jets [7]	D0 dilepton [8]
Statistical	0.039	0.11	0.027	0.056
Background	0.022	0.04	0.010	0.007
Signal	0.011	0.05	0.005	0.026
Detector	0.007	0.02	0.003	0.001
Method	0.004	0.02	0.005	0.014
PDF	0.001	0.01	0.004	0.003

Table 2: Inputs to and results from the combination of the $t\bar{t}$ asymmetries.

Analysis	$A_{\mathrm{FB}}^{t\bar{t}}$	Uncertainty			Weight
		Stat.	Syst.	Total	
CDF ℓ+ jets [6]	0.164	0.039	0.026	0.047	0.25
CDF dilepton [9]	0.12	0.11	0.07	0.13	0.01
D0 ℓ+ jets [7]	0.106	0.027	0.013	0.030	0.64
D0 dilepton [8]	0.175	0.056	0.031	0.063	0.11
Combination	0.128	0.021	0.014	0.025	

Table 3: The statistical and systematic uncertainties in the individual $A_{\rm FB}^{\ell}$ inputs. The D0 PDF uncertainty for the dilepton channel was not evaluated but is estimated to be negligible.

Uncertainty	CDF ℓ+ jets [11]	CDF dilepton [14]	D0 ℓ+ jets [12]	D0 dilepton [13]
Statistical	0.024	0.052	0.027	0.037
Background	0.015	0.029	$^{+0.016}_{-0.018}$	0.008
Signal	0.0074	negligible	0.008	0.005
Detector	0.0022	0.004	$^{+0.008}_{-0.011}$	0.005
Method	$^{+0.013}_{-0.000}$	0.006	0.008	0.004
PDF	0.0025	negligible	0.002	

The differential $t\bar{t}$ asymmetries as a function of Δy and $m_{t\bar{t}}$ are plotted separately for each channel and experiment in Fig. 1, as well as their NNLO theoretical predictions [10].

4 $A_{\rm FB}^{\ell}$ combination

The uncertainties in each of the $A_{\rm FB}^{\ell}$ measurements are summarized in Table 3, where we include in the "method" category the uncertainty in the D0 modeling extrapolated to the unmeasured part of the phase space. The CDF and D0 $A_{\rm FB}^{\ell}$ input values and their combination using BLUE in the ℓ + jets and dilepton channels are shown in Table 4, together with the statistical, systematic, and total uncertainties, as well as the weights from each measurement contributing to the combination. The resulting $A_{\rm FB}^{\ell} = 0.073 \pm 0.020$ has a χ^2 of 2.17 for 3 degrees of freedom, for a probability of 54%, which is consistent within 1.6 standard deviations with the NLO SM prediction of 0.038 ± 0.003 [2].

The differential single lepton asymmetries as a function of $q_\ell \eta_\ell$ are plotted separately for each channel and experiment in Fig. 2.

5 $A_{\rm FB}^{\ell\ell}$ combination

The uncertainties in each of the $A_{\rm FB}^{\ell\ell}$ measurements are summarized in Table 5. The CDF and D0 $A_{\rm FB}^{\ell\ell}$ inputs and their combination using BLUE in the dilepton channel are shown in Table 6, together with the statistical, systematic, and total uncertainties, as well as the weights from each measurement contributing to the combination. The resulting $A_{\rm FB}^{\ell\ell} = 0.108 \pm 0.046$ has a χ^2 of 0.22 for 1 degree of

Table 4: Inputs to and results from the combination of the single lepton asymmetries.

Analysis	$A_{\rm FB}^{\ell}$	Uncertainty			Weight
		Stat.	Syst.	Total	
CDF ℓ+ jets [11]	0.105	0.024	$^{+0.022}_{-0.017}$	$^{+0.032}_{-0.029}$	0.40
CDF dilepton [14]	0.072	0.052	0.030	0.060	0.11
D0 ℓ+ jets [12]	0.050	0.027	$^{+0.020}_{-0.024}$	$^{+0.034}_{-0.037}$	0.27
D0 dilepton [13]	0.044	0.037	0.011	0.039	0.23
Combination	0.073	0.016	0.012	0.020	

freedom, for a probability of 64%, which is consistent within 1.3 standard deviations with the NLO SM prediction of 0.048 ± 0.004 [2]. The differential dilepton asymmetries as a function of $\Delta\eta$ are plotted separately for each experiment in Fig. 3.

Table 5: The statistical and systematic uncertainties in the individual $A_{\rm FB}^{\ell\ell}$ inputs. The D0 PDF uncertainty for the dilepton channel was not evaluated but is estimated to be negligible.

Uncertainty	CDF dilepton [14]	D0 dilepton [13]
Statistical	0.072	0.054
Background	0.037	0.009
Signal	negligible	0.009
Detector	0.003	0.006
Method	0.013	0.004
PDF	negligible	

6 Summary

The CDF and D0 measurements are in fairly good agreement with each other as indicated by the χ^2 values of the combinations. The combined results of the CDF and D0 measurements of the inclusive $t\bar{t}$ asymmetries $A_{\rm FB}^{t\bar{t}}$, $A_{\rm FB}^{\ell}$, and $A_{\rm FB}^{\ell\ell}$ are:

$$A_{\rm FB}^{t\bar{t}} = 0.128 \pm 0.025 \ [\pm 0.021(\text{stat.}) \pm 0.014(\text{syst.})] \ , \quad (4)$$

$$A_{\rm FB}^{\ell} = 0.073 \pm 0.020 \ [\pm 0.016(\text{stat.}) \pm 0.012(\text{syst.})] \ , \quad (5)$$

$$A_{\rm FB}^{\ell\ell} = 0.108 \pm 0.046 \ [\pm 0.043(\text{stat.}) \pm 0.016(\text{syst.})] \ . \quad (6)$$

Table 6: Inputs to and results from the combination of the dilepton lepton asymmetries.

Analysis	$A_{\rm FB}^{\ell\ell}$	Uncertainty			Weight
		Stat.	Syst.	Total	
CDF dilepton [14]	0.076	0.072	0.037	0.082	0.32
D0 dilepton [13]	0.123	0.054	0.015	0.056	0.68
Combination	0.108	0.043	0.016	0.046	

The corresponding SM predictions are $A_{\rm FB}^{t\bar{t}} = 0.095 \pm 0.007$, $A_{\rm FB}^{\ell} = 0.038 \pm 0.003$, and $A_{\rm FB}^{\ell\ell} = 0.048 \pm 0.004$. The three asymmetries are correlated to some extent since a positive rapidity difference between a t and a $\bar{t}$ quark is likely to result in a positive pseudorapidity difference between a positive and negative decay lepton. The results are summarized in Fig. 4. The differential asymmetries are shown in Figures 1, 2, and 3. The measurements are in agreement with the existing predictions of the SM.

7 Acknowledgements

We thank the Fermilab staff and the technical staffs of the participating institutions for their vital contribnutinos. This work was supported by DOE and NSF (USA), CONICET and UBACyT (Argentina), ARC (Australia), CNPq and FAPERJ (Brazil), NSERC Canada), CAS and CNSF (China), Colciencias (Colombia), MSMT (Czech Republic), Marie Curie Fellowship Contract No. 3023103 (EU Community), Academy of Finland (Finland), CEA and CNRS/IN2P3 (France), BMBF and DFG (Germany), DAE and DST (India), SFI (Ireland), INFN (Italy), MEXT (Japan), NRD (Korea), CONACyT (Mexico), NSC (Republic of China), MON, NRC, KI and RFBR (Russia), Slovak R&D Agency (Slovakia), Ministerio de Ciencia e Innovaci'on and Programa Consolider-Ingenio 2010 (Spain), Swedish Research Council (Sweden), Swiss National Science Foundation (Switzerland), FOM (The Netherlands), MESU (Ukraine), STFC and The Royal Society (UK), and the A.P. Sloan Foundation (USA).

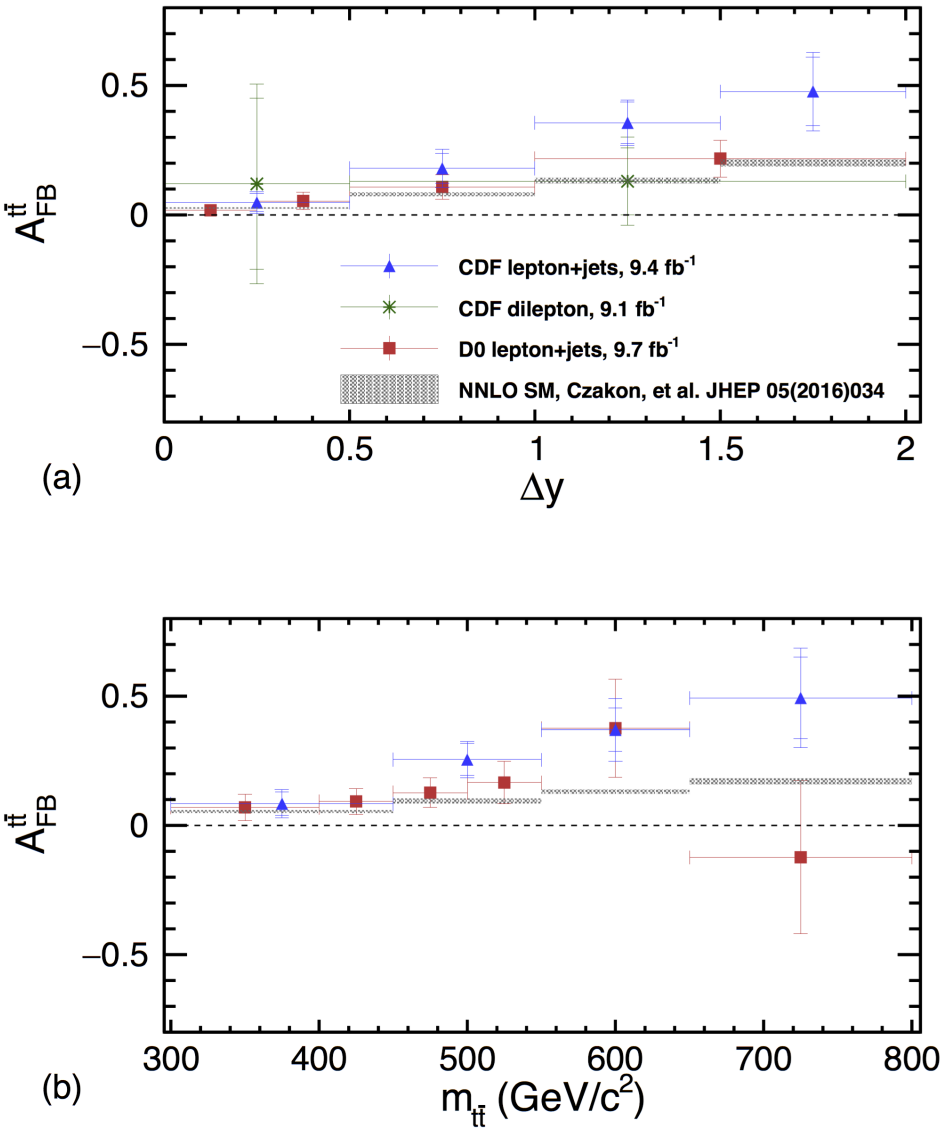

Figure 1: Comparison of the differential asymmetries $A_{\rm FB}^{t\bar{t}}$ as a function of (a) Δy and (b) $m_{t\bar{t}}$.

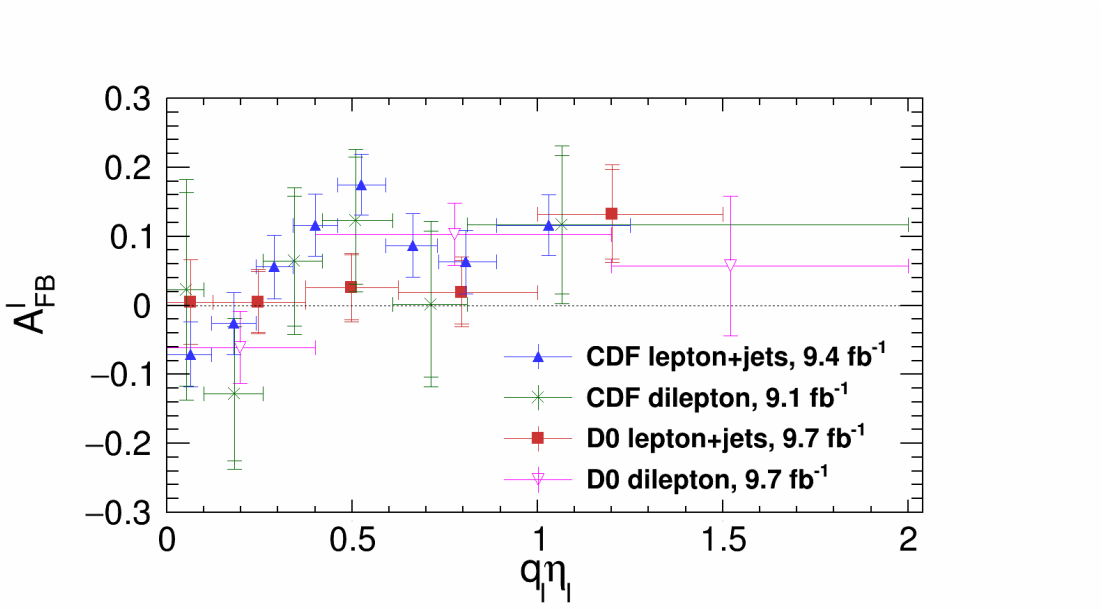

Figure 2: Comparison of the differential asymmetries $A^{\ell}_{\rm FB}$ as a function of $q_\ell \eta_\ell$.

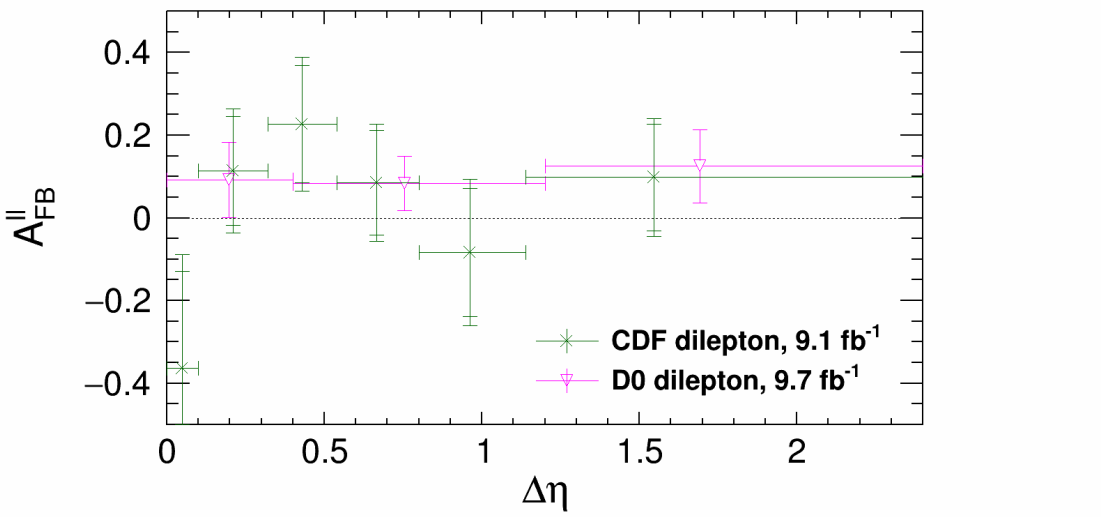

Figure 3: Comparison of the differential asymmetries $A^{\ell\ell}_{\rm FB}$ as a function of $\Delta\eta$.

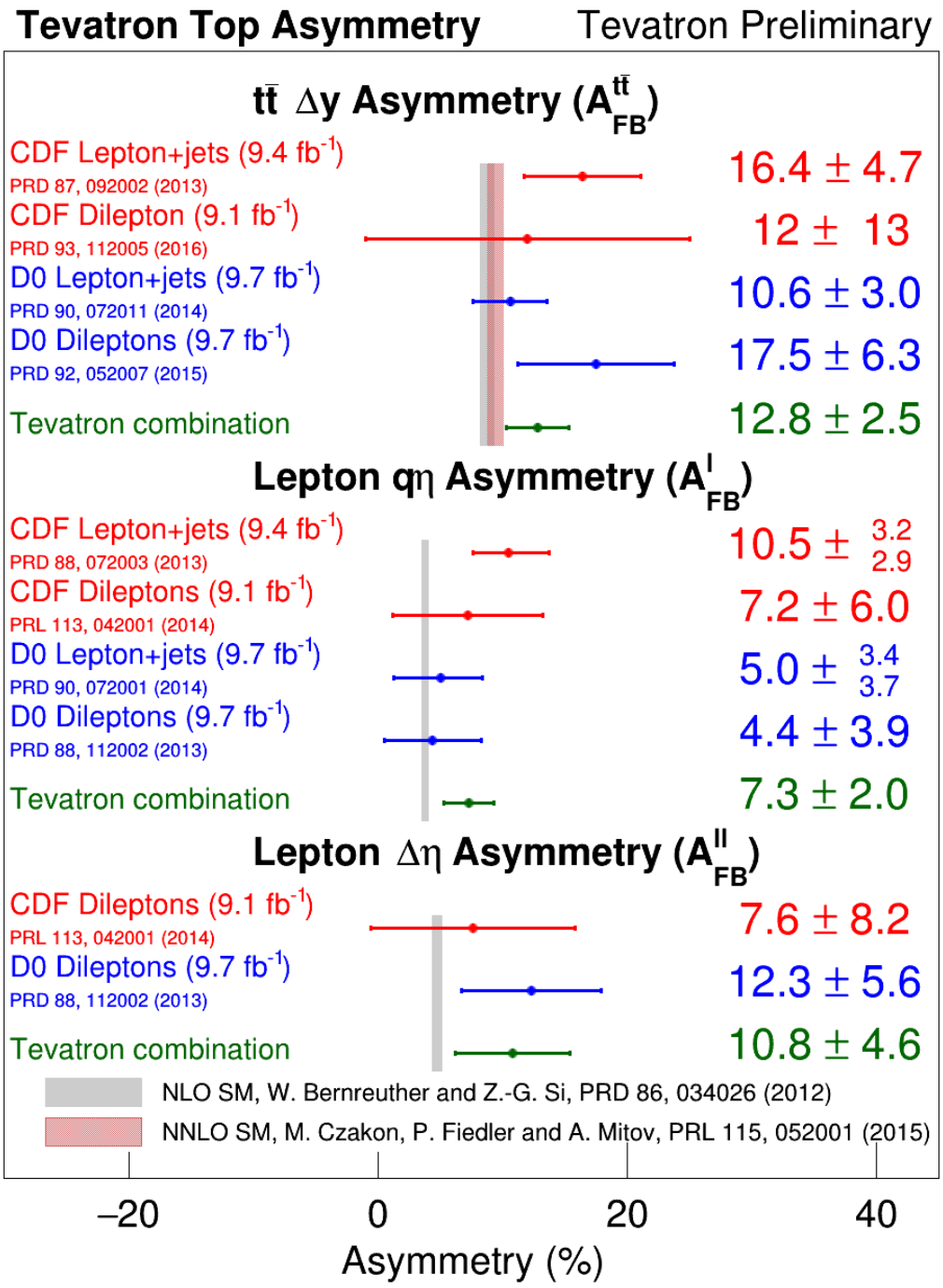

Figure 4: Summary of inclusive top forward–backward asymmetries in $t\bar{t}$ events measured at the Tevatron. Values are provided in %, while for all other instances in this document we provide fractions.

References

[1] M. Czakon, P. Fiedler and A. Mitov, Phys. Rev. Lett. **115**, 052001 (2015).

[2] W. Bernreuther and Z.-G. Si, Phys. Rev. D **86**, 034026 (2012).

[3] D. Acosta *et al.*, (CDF Collaboration), Phys. Rev. D **71** ,032001 (2005)

[4] V.M. Abazov *et al.*, (D0 Collaboration), Nucl. Instr. Methods Phys. Res. A **565**, 463 (2006).

[5] J.A. Aguilar-Saavedra, D. Amidei, A. Juste, and M. Pérez-Victoria, Rev. Mod. Phys. **87**, 421 (2015).

[6] T. Aaltonen *et al.*, (CDF Collaboration), Phys. Rev. D **87**, 092002 (2013).

[7] V.M. Abazov *et al.*, (D0 Collaboration), Phys. Rev. D **90**, 072011 (2014).

[8] V.M. Abazov *et al.*, (D0 Collaboration), Phys. Rev. D **92**, 052007 (2015).

[9] T. Aaltonen *et al.*, (CDF Collaboration), Phys. Rev. D **93**, 112005 (2016).

[10] M. Czakon, P. Fiedler, D. Heymes, A. Mitov, J. High Energy Phys. **05**, 034 (2016).

[11] T. Aaltonen *et al.*, (CDF Collaboration), Phys. Rev. D **88**, 072003 (2013).

[12] V.M. Abazov *et al.*, (D0 Collaboration), Phys. Rev. D **90**, 072001 (2014).

[13] V.M. Abazov *et al.*, (D0 Collaboration), Phys. Rev. D **88**, 112002 (2013).

[14] T. Aaltonen *et al.*, (CDF Collaboration), Phys. Rev.Lett. **113**, 042001 (2014).

[15] L. Lyons, D. Gibaut and P. Clifford, Nucl. Instrum. Meth. A **270**, 110 (1988).

[16] L. Lyons, A.J. Martin and D.H. Saxon, Phys. Rev. D **41**, 982 (1990).

[17] A. Valassi, Nucl. Instrum. Meth. A **500**, 391 (2003).